Stephan Allgeier*, Fabian Anzlinger, Sebastian Bohn, Ralf Mikut, Oliver Neumann, Klaus-Martin Reichert, Oliver Stachs, and Karsten Sperlich

An open-source software for the simulation of fixational eye movements

https://doi.org/10.1515/cdbme-2024-2007

Abstract: Laser-scanning confocal microscopy of the human cornea acquires *in vivo* images of corneal tissues with cellular resolution, which offers diagnostic potential for a variety of diseases. However, involuntary fixational eye movements induce motion artefacts that pose a challenge for accurate morphometric analysis and particularly for preceding image data fusion steps. Different image registration algorithms promise to eliminate such artefacts, but objective, quantitative evaluation of the registration results is difficult because of the lack of ground truth data. Simulation approaches offer a possibility to close this gap. Existing open-source software for the simulation of fixational eye movements is currently limited to creating drift movement. The present contribution proposes complementary models for microsaccade and tremor components to provide complete simulated fixational eye movement paths. In addition, it reports results from an extensive examination of different model parameter combinations. It is shown that the microsaccade model is capable of reproducing intermicrosaccade intervals that closely resemble experimental data. A software implementation is provided as open-source Python modules.

Keywords: fixational eye movements, microsaccades, tremor, simulation, open source software

1 Introduction

Laser-scanning confocal microscopy (LSCM) of the human cornea is a non-invasive imaging technique to obtain high-resolution *in vivo* images of the corneal tissues and cellular structures. Regarding the image sampling process and the available frame rates in LSCM, any movement of the imaged scene induces motion artefacts in the recorded image data. This is particularly relevant in the ophthalmological context, as the eyes are generally constantly in motion, even during conscious static fixation.

These fixational eye movements (FixEM) are involuntary and cannot be suppressed willingly. Three components of FixEM are distinguished: microsaccades, drift and tremor [1]. The high-frequency, low-amplitude tremor appears as a jitter overlaying the continuous, slow, low-frequency drift movement. The drift is sporadically interrupted by fast ballistic, high-amplitude microsaccades.

The motion artefacts caused by FixEM are a major challenge for any downstream processing tasks of LSCM data. Especially for image data fusion of LSCM image sequences — e.g. for 2D montages of the corneal sub-basal nerve plexus [2], or for volume reconstructions from depth scans [3] — the algorithmic removal of motion artefacts is crucial for high-quality results. Different image registration algorithms have been developed to align LSCM image data and correct motion-induced distortions [3].

One approach towards quantitative evaluation of the LSCM image registration algorithms is to apply them to image datasets with known ground truth. This can be accomplished in a simulation environment where the images are computationally generated using a given scene and motion path. Alternatively, the image data can be acquired within a well-controlled experimental setup with a stage capable of performing the required movements. Both approaches need a motion trajectory as input. To that end, Nau et al. have developed the open-source framework *Eye Motion Simulation* [4] that simulates drift trajectories. However, with respect to the evaluation of LSCM image registration algorithms, the lack of microsaccades is a particular limitation because they cause severe motion artefacts, and the LSCM imaging process generally takes several seconds, so capturing datasets without microsaccades is not a viable option.

The purpose of the present contribution is to extend the *Eye Motion Simulation* framework with functionality for microsaccades and tremor. It further presents results of an extensive examination of the simulation parameters and provides a parameter set for realistic FixEM trajectories. A Python implementation of the proposed methods is available in the open-source *FixEM Simulator* [5].

***Corresponding author: Stephan Allgeier,** Karlsruhe Institute of Technology (KIT), Institute for Automation and Applied Informatics, Karlsruhe, Germany, e-mail: stephan.allgeier@kit.edu
Fabian Anzlinger, Ralf Mikut, Oliver Neumann, Klaus-Martin Reichert, Karlsruhe Institute of Technology (KIT), Institute for Automation and Applied Informatics, Karlsruhe, Germany
Sebastian Bohn, Oliver Stachs, Karsten Sperlich, Rostock University Medical Center, Department of Ophthalmology, Rostock, Germany

2 Fundamentals

In [6], Engbert et al. proposed a mathematical model to simulate FixEM. It defines a dynamic potential field over a confined 2D region that represents the gaze direction. The potential field is defined over a discrete, square grid of $L \times L$ cells that covers the region of $\pm 1^\circ$ of visual angle from the central fixation direction. The model consists of a drift generator that is driven by the dynamic potential field, and a mechanism to trigger microsaccades. The authors showed that the simulated FixEM trajectories reproduce important characteristics of real FixEM paths.

For the drift simulation in the open-source *Eye Motion Simulation* framework [4], Nau et al. adapted the drift component of Engbert's model. One of the original contributions of their adaptation was the translation of the model to create drift trajectories over a continuous space instead of a discrete grid.

The following brief overview of the mentioned drift and microsaccade models focuses on the aspects that are relevant to the new contributions proposed in section 3.

2.1 Drift Model

The drift model implemented in the *Eye Motion Simulation* framework [4] uses the so-called self-avoiding random walk in a potential field. The iterative algorithm creates a discrete sequence of gaze directions that are guided to lower values in the potential field. The potential field consists of a static, continuous fixation potential

$$u\left(x,y\right) = \lambda \cdot \left(\left(x-x_0\right)^2 + \left(y-y_0\right)^2\right) \tag{1}$$

with a weight factor λ and the central fixation direction (x_0, y_0), and a dynamic activation potential $h_t\left[i,j\right]$ that is represented in a discrete grid over the considered area.

Every step is determined by first randomly sampling a number of step vector candidates with uniformly distributed directions and normally distributed lengths with mean μ_{step} and standard deviation σ_{step}. Each step candidate is then assigned a probability based on the fixation potential u at the target position of the step, the activation potential h_t of all grid cells that the step traverses, and a weight constant w_{pot} that determines the influence of the potential field on the step vector selection. Given the candidate probabilities, a step vector is finally sampled from the set of candidates by weighted random selection. After each step, the activation potential $h_t\left[i,j\right]$ is incremented by 1 for all grid cells traversed by the step and decreased by a relaxation rate ϵ in all other grid cells.

All calculated points along the path are considered to be spaced equally in time; the variable step lengths represent changes in drift velocity. The simulation frequency f_{sim} defines the time interval between the sample points.

2.2 Microsaccade Model

In [6], the authors observed that their initial drift model generates trajectories that largely remain in the central area of the grid, even though this leads to a constantly increased activation level in that region. The small steps will not direct the random walk into the periphery of the grid despite lower values of the potential field in these regions. The purpose of the microsaccades would be to force the gaze trajectory into these low-potential areas. The authors, therefore, introduced a microsaccade generation threshold h_{crit}. A microsaccade is triggered whenever the activation value $h_t\left[i_t,j_t\right]$ at the current grid cell $[i_t,j_t]$ exceeds h_{crit}. Since there exists evidence in recorded human FixEM trajectories that microsaccades have a strong preference to follow a purely horizontal or purely vertical direction over mixed directions, a third potential was introduced, the oculomotor potential

$$u_{dir,t}\left[i,j\right] = \chi \cdot \left(\left(i-i_t\right)^2 \cdot \left(j-j_t\right)^2\right) \tag{2}$$

with a weight factor χ. The target point of the microsaccade is then simply the grid cell with the overall lowest sum potential $h_t + u + u_{dir,t}$.

3 Methods

The overarching aim of the work presented herein is to provide an open-source software to simulate FixEM that include all three components. To this end, the *Eye Motion Simulation* framework [4] is used as a basis. This section proposes extensions that add the missing functionality for microsaccades and tremor components.

3.1 Microsaccade Extension

The microsaccade generator that is proposed here follows the basic ideas described in section 2.2. However, instead of operating on a discrete grid, it needs to be adapted to the continuous-space implementation of the *Eye Motion Simulation* framework. This adaptation is implemented as a two-step process as follows.

During the drift movement (see section 2.1), the microsaccade generator is triggered whenever the activation

potential $h_t\,[i_t, j_t]$ of the cell, in which the current trajectory point (x_t, y_t) is located, exceeds the threshold level h_{crit}. In the first step, the discrete target cell is determined as the cell with the lowest overall potential sum

$$h_t\,[i,j] + u\,[i,j] + u_{dir,t}\,[i,j]\,. \tag{3}$$

Note that the fixation potential u is actually defined as a continuous function in eq. (1). For the purpose of eq. (3), $u\,[i,j]$ is calculated as the fixation potential value at the central point of the grid cell $[i,j]$. In the second step, the exact target position of the microsaccade inside the target cell is determined. This is implemented by sampling a large number of (uniformly distributed) random points (x', y') inside the target cell, calculating the potential sum

$$u\left(x', y'\right) + u_{dir,t}\left(x', y'\right) \tag{4}$$

and selecting the point with the lowest sum value as the actual target point of the microsaccade. The activation potential h is omitted here because it has the same value for all points inside the target cell. The oculomotor potential u_{dir}, on the other hand, is calculated with continuous coordinates for the purpose of eq. (4). The definition is identical to eq. (2) but the discrete grid coordinates $[i,j]$ are replaced by the continuous coordinates (x,y).

Now that the microsaccade step vector is known, its duration or velocity remains to be specified. Simply assuming the microsaccade duration to be the same as the time interval of a drift step could lead to unrealistic microsaccade duration and velocity values. In order to avoid this, the duration is explicitly determined for each microsaccade by independent random sampling from a uniform distribution over the interval between 10 ms and 20 ms. Depending on the simulation frequency f_{sim}, this may necessitate the calculation of several additional trajectory points along the microsaccade path. In this case, these points are determined by linear interpolation between the microsaccade start and end point.

3.2 Tremor Extension

The published amplitude values of the high-frequency tremor vary strongly [1]; a more recent examination reports them to be in the range of 1 to 5 arcseconds [7]. Since the tremor has only a minor influence on the motion artefacts in LSCM image data, the proposed tremor model is very simple. It generates independent deviation vectors for the trajectory points, which are added to the calculated path coordinates. Only points during drift segments are modified in order to keep the constant direction of the ballistic microsaccades. The x- and y-components of the tremor vectors are sampled from a normal distribution with mean 0 and a standard deviation of $3\sigma = 5 \cdot (2)^{-0.5}$. Thus, approx. 99.7 % of the calculated tremor vectors will have a length of $\leq$5 arcseconds.

4 Experiments and Results

The drift model and the microsaccade extension described above are controlled by several parameters that require careful adjustment. An extensive experimental analysis of different parameter combinations has been performed in order to identify settings that generate realistic FixEM paths. As the focus of the present contribution is on the microsaccade extension, the distribution of the intermicrosaccade intervals (IMSI) has been chosen as the primary metric to evaluate the generated FixEM paths.

Four parameters have been identified to have the strongest influence on the microsaccade generation: the simulation frequency f_{sim}, the grid size L of the dynamic activation potential, the relaxation rate ϵ, and the activation level threshold h_{crit} that triggers a microsaccade. To limit the search space, only these four parameters have been varied using the following values:

- $f_{sim} = 100\,;\ 150\,;\ 200\,;\ 250\,\mathrm{Hz}$
- $L = 21\,;\ 51\,;\ 101\,;\ 201\,;\ 301$
- $\epsilon = 0.001\,;\ 0.002\,;\ 0.005\,;\ 0.01\,;\ 0.015\,;\ \ldots\,;\ 0.095\,;\ 0.1$
- $h_{crit} = 1.9\,;\ 2.4\,;\ 2.9\,;\ \ldots\,;\ 9.4\,;\ 9.9$

All other parameters have been set to constant values and remained unchanged. The following settings have been used for the examination: A field of view of $\pm 1°$, weight constants $\lambda = 1$, $\chi = 1$ and $w_{pot} = 5$, and a mean and standard deviation for the drift step vector sampling of $\mu_{step} = 0.05°$ and $\sigma_{step} = 0.01°$, respectively.

The specified parameter value ranges result in a total of 7480 examined combinations. Each combination has been tested as follows. 25 trajectories of 30 seconds were generated. The first 10 seconds were removed from each trajectory because the activation potential needs to build up first before microsaccades are triggered regularly. The IMSI from the 25 repetitions were extracted and combined. For a qualitative and quantitative evaluation, the IMSI statistics and histogram were compared with real-world data from the Roorda Lab dataset [7]. The evaluation of the resulting IMSI distributions was based on the IMSI median (m_{imsi}), mean (μ_{imsi}), and standard deviation, (σ_{imsi}). It also used the absolute histogram difference $D_{hist} = \sum_{b \in B} |H_S\,(b) - H_R\,(b)|$ as a similar-

Tab. 1: Parameter combinations with the lowest associated absolute histogram difference D_{hist}.

Parameters				IMSI statistics			
f_{sim} [Hz]	L	ϵ	h_{crit}	m_{imsi} [s]	μ_{imsi} [s]	σ_{imsi} [s]	D_{hist}
150	21	0.085	8.9	0.393	0.572	0.582	3.969
150	21	0.100	8.4	0.407	0.619	0.641	4.093
100	21	0.100	6.9	0.500	0.772	0.775	4.103
150	21	0.090	8.9	0.427	0.638	0.642	4.161
100	21	0.095	6.9	0.460	0.708	0.737	4.183
Roorda Lab dataset				0.526	0.737	0.755	

ity measure, where H_S and H_R are the IMSI histograms derived from the simulations and from the Roorda Lab dataset, respectively, both using the same set of bins B with a bin size of 50 ms. Table 1 lists the five best parameter combinations in terms of D_{hist}.

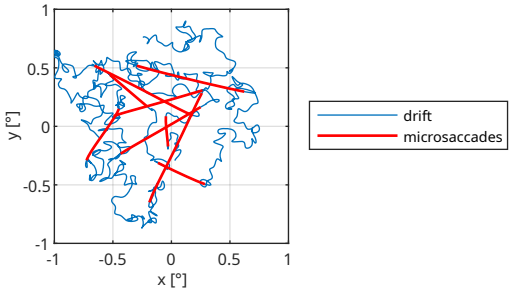

Fig. 1: Section (3 seconds) of a simulated FixEM trajectory.

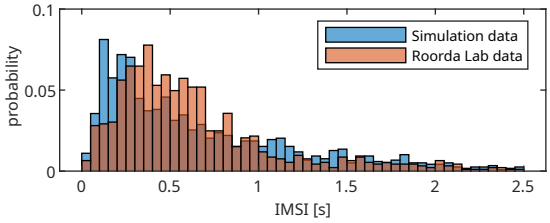

Fig. 2: Histogram comparison of simulated and real IMSI data.

5 Discussion

The results listed in Table 1 show that the proposed simulation model is able to generate FixEM trajectories with drift and microsaccades that manifest IMSI distributions similar to those found in eye-tracking datasets. Figure 1 shows 3 seconds of an exemplary simulated FixEM trajectory that has been generated with the third set of parameters in Table 1; this parameter combination recreates the IMSI median, mean, and standard deviation of the Roorda Labs dataset particularly closely. Figure 2 shows the corresponding IMSI distribution histogram. It reveals small deviations, especially at the low end — very short IMSI durations are overrepresented to some degree in the simulated data. The other parameter combinations in Table 1 show the same effect. The reason for the small deviations in the simulated IMSI distribution from the experimental data is currently being analysed. Further and more fine-grained parameter adjustments might alleviate the effect. Also, Figure 1 suggests that the weight χ needs to be increased to generate a more realistic angle distribution with more horizontal and vertical microsaccades.

In conclusion, the present contribution describes mathematical models for the simulation of microsaccades and tremor within an existing drift simulation framework. This contribution also provides a set of control parameters that produces microsaccades in realistic time intervals. The complete software framework is made available as open-source Python modules in the *FixEM Simulator* project [5].

Author Statement

Research funding: Parts of the work were funded by the Deutsche Forschungsgemeinschaft (DFG, German Research Foundation) – project number 469107515.
Conflict of interest: Authors state no conflict of interest.
Informed consent/Ethical approval: The conducted research is not related to either human or animal use.

References

[1] Martinez-Conde S, Macknik SL, Hubel DH. The role of fixational eye movements in visual perception. Nat Rev Neurosci 2004;5:229–240.
[2] Allgeier S, Bartschat A, Bohn S, Guthoff RF, Hagenmeyer V, Kornelius L, et al. Real-time large-area imaging of the corneal subbasal nerve plexus. Sci Rep 2022;12:2481.
[3] Bohn S, Sperlich K, Allgeier S, Bartschat A, Prakasam R, Reichert KM, et al. Cellular in vivo 3D imaging of the cornea by confocal laser scanning microscopy. Biomed Opt Express 2018;9:2511–2525.
[4] Nau MA, Ploner SB, Moult EM, Fujimoto JG, Maier AK. Open source simulation of fixational eye drift motion in OCT scans. In: Tolxdorff T, Deserno T, Handels H, Maier A, Maier-Hein K, Palm C, editors. Bildverarbeitung für die Medizin 2020. Wiesbaden: Springer Vieweg; 2020:254–259.
[5] Anzlinger F, Allgeier S. FixEM Simulator. GitLab repository. Available: https://gitlab.kit.edu/kit/iai/ml4time/cornea/FixEM-Simulator.
[6] Engbert R, Mergenthaler K, Sinn P, Pikovsky A. An integrated model of fixational eye movements and microsaccades. Proc Natl Acad Sci U S A 2011;108:E765–770.
[7] Bowers NR, Boehm AE, Roorda A. The effects of fixational tremor on the retinal image. J Vis 2019;19:8.